Supporting Information for: Processing Methods for Obtaining a Face-On Crystalline Domain Orientation in Conjugated Polymer-Based Photovoltaics

Taylor J. Aubry,[1,†] Amy S. Ferreira,[1,†] Patrick Y. Yee,[1] Jordan C. Aguirre,[1] Steven A. Hawks,[2] Matthew T. Fontana,[1] Benjamin J. Schwartz,[1,3,*], and Sarah H. Tolbert[1,2,3,*]

[1]Department of Chemistry and Biochemistry, University of California, Los Angeles, Los Angeles, California 90095-1569, United States

[2]Department of Materials Science and Engineering, University of California, Los Angeles, Los Angeles, California 90095-1569, United States

[3]California NanoSystems Institute, University of California, Los Angeles, Los Angeles, California 90095-1569, United States

*Corresponding Authors E-mail: tolbert@chem.ucla.edu, schwartz@chem.ucla.edu
[†]TJA and ASF contributed equally to this work.

I. Experimental details

The polymer poly[4,8-bis-(2-ethylhexyloxy)-benzol[1,2-b:4,5-b']dithiophene-2,6-diyl-alt-4-(2-ethylhexyloxy-1-one)thieno[3,4-b]thiophene-2,6-diyl] (PBDTTT-C) and [6,6]-phenyl-C_{71}-butyric-acid-methylester ($PC_{71}BM$) were purchased from Solarmer and used as received. All devices were fabricated on indium tin oxide (ITO) substrates (150 nm, 20 Ω/□) that were sequentially sonicated in baths of detergent, water, acetone, and isopropyl alcohol followed by UV ozone treatment for 20 minutes. Subsequently, 35 nm of poly(ethylenedioxythiophene): poly(styrenesulfonic acid) (PEDOT:PSS Clevios PVP AI 4083) was deposited onto the ITO to form the hole collection layer and baked at 150 °C for 20 minutes. For the blend-cast devices, the 1:1.5 wt/wt PBDTTT-C:$PC_{71}BM$ solution was deposited at 1800 rpm for 60 s. For sequentially processed devices, the polymer solution was spun at 2500 rpm for 60 s followed by deposition of the fullerene solution onto the fully dry polymer layer at 2000 rpm for 60 s. Pure polymer films for grazing-incidence wide-angle X-ray scattering (GIWAXS) and space-charge limited current (SCLC) studies were deposited at the same conditions as the first SqP step. Methanol (MeOH) washing of devices containing 3% v/v 1,8-diiodooctane (DIO) was performed at 4000 rpm for 10 s. After deposition of the active layer, both blend-cast and sequentially-processed films were fabricated into devices by thermally evaporating 10 nm of Ca and 70 nm of Al as cathodes at a pressure of 1×10^{-6} Torr using an Ångstrom Engineering NexDep evaporator. The Ca layer was deposited at a rate of 0.5 Å/s to a thickness of 10 nm, and the Al layer was deposited at a rate of 1.5 Å/s to a thickness of 80 nm. Before exposing the devices to the metals, ~10 nm of Ca was evaporated onto the shutter to ensure layer purity. For SCLC diodes Au was evaporated at a rate of 0.5 Å/s for the first 10 nm and then at 1 Å/s to a final thickness of 60 nm.

II. Polymer crystallite coherence length in pure, blend cast and sequentially processed films

Table S1. Summary of (100) peak location, integrated peak area, and coherence length as calculated from the Scherrer equation.

Sample		100 Location ($Å^{-1}$)	Relative Peak Area	Error	Coherence length (nm)	Error
Pure PBDTTT-C	no DIO	0.34	1.0	0.3	4.1	0.1
	w/ DIO	0.32	1.6	0.3	3.7	0.4
	w/ DIO + MeOH wash	0.33	1.5	0.4	3.8	0.4
Blend Cast BHJ	no DIO	0.36	2.0	0.6	2.4	0.1
	w/ DIO	0.36	1.4	0.4	3.9	0.8
	w/ DIO + MeOH wash	0.39	2.8	0.4	3.1	0.1
Sequentially Processed BHJ	no DIO	0.35	2.1	0.3	4.9	0.3
	w/ DIO	0.34	1.7	0.5	5.7	0.1

The (100) crystallite coherence lengths were calculated by peak fitting the fully integrated diffractograms and using the Scherrer equation $\tau = \frac{K\lambda}{\beta cos\theta}$ where τ is the coherence length, K is the dimensionless shape factor taken to be 0.9, λ is the X-ray wavelength 0.9742 Å, β is the FWHM of the fit and θ is the peak location.

III. Solvent effects on pure PBDTTT-C

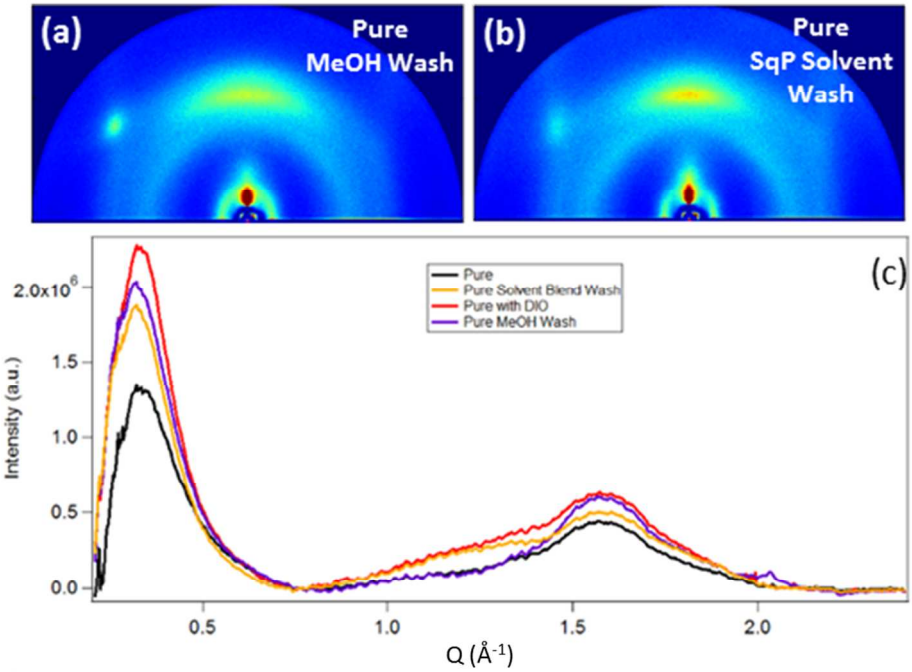

Figure S1. 2D-GIWAXS of pure PBDTTT-C films after washing with methanol (a) and 1:1 2-chlorophenol:dicholoromethane (b), which was used to deposit the fullerene during sequential processing. Fully integrated diffractograms (c) for pure polymer (black), polymer with DIO (red), and pure polymer washed with methanol (purple) and the SqP solvent blend (orange). An increase in crystallinity over pure is observed with each of the pure solvent washes, however the addition of DIO causes the largest change.

IV. Effect of methanol washing on blend-cast PBDTTT-C:$PC_{71}BM$ with and without DIO

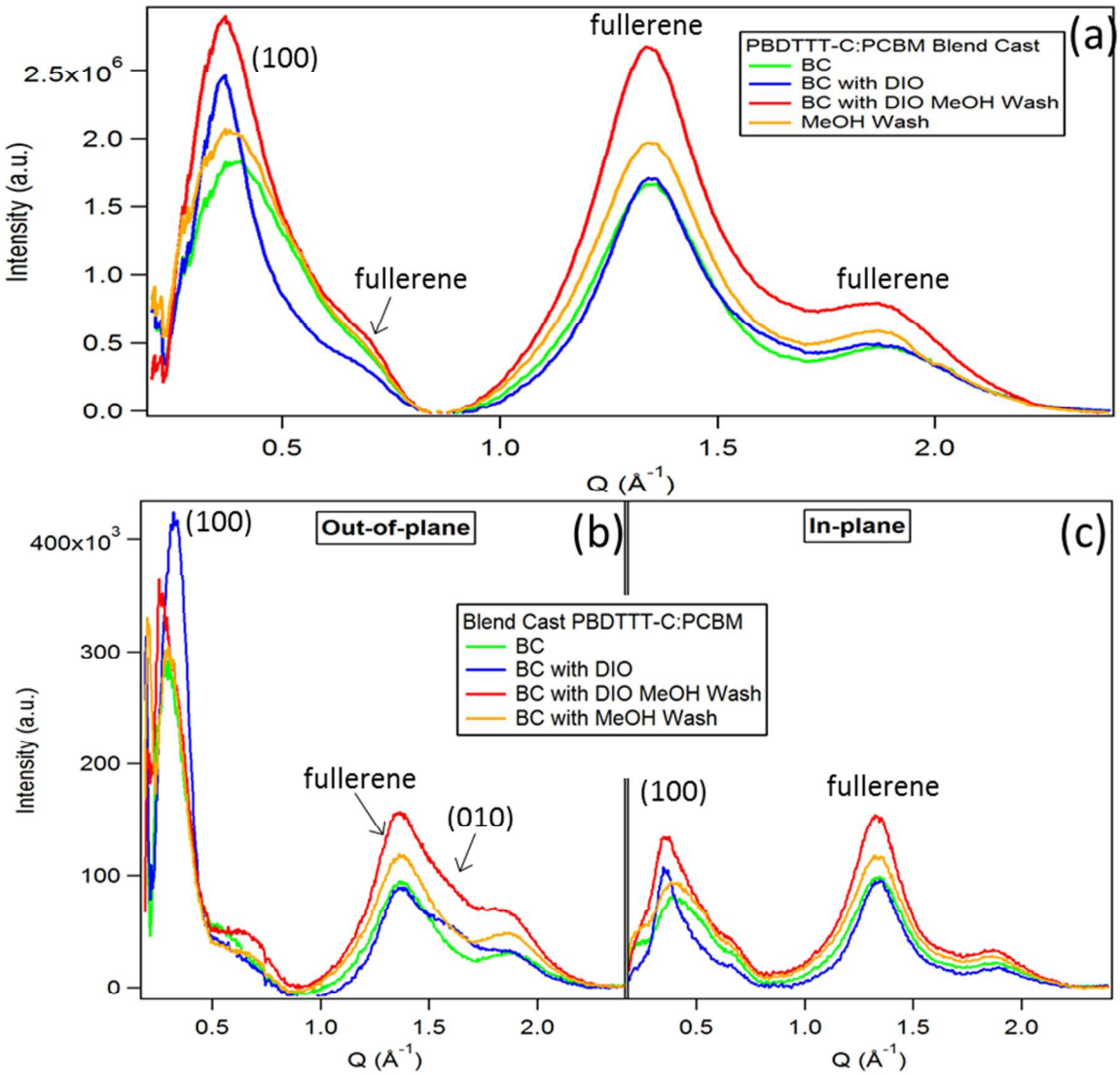

Figure S2. Examination of the role of methanol washing only for BC devices. (a) Full integration of GIWAXS diffractograms for 1:1.5 PBDTTT-C:PCBM blend cast (BC) films without (green), with 3% DIO (blue), and subsequent methanol wash (red). Methanol wash of a blend cast film without DIO (orange) shows little change. Isotropic fullerene orientation is observed by the equal intensity (b) out-of-plane and (c) in-plane.

V. Sequentially processed PBDTTT-C:$PC_{71}BM$ (10 mg/mL PCBM concentration)

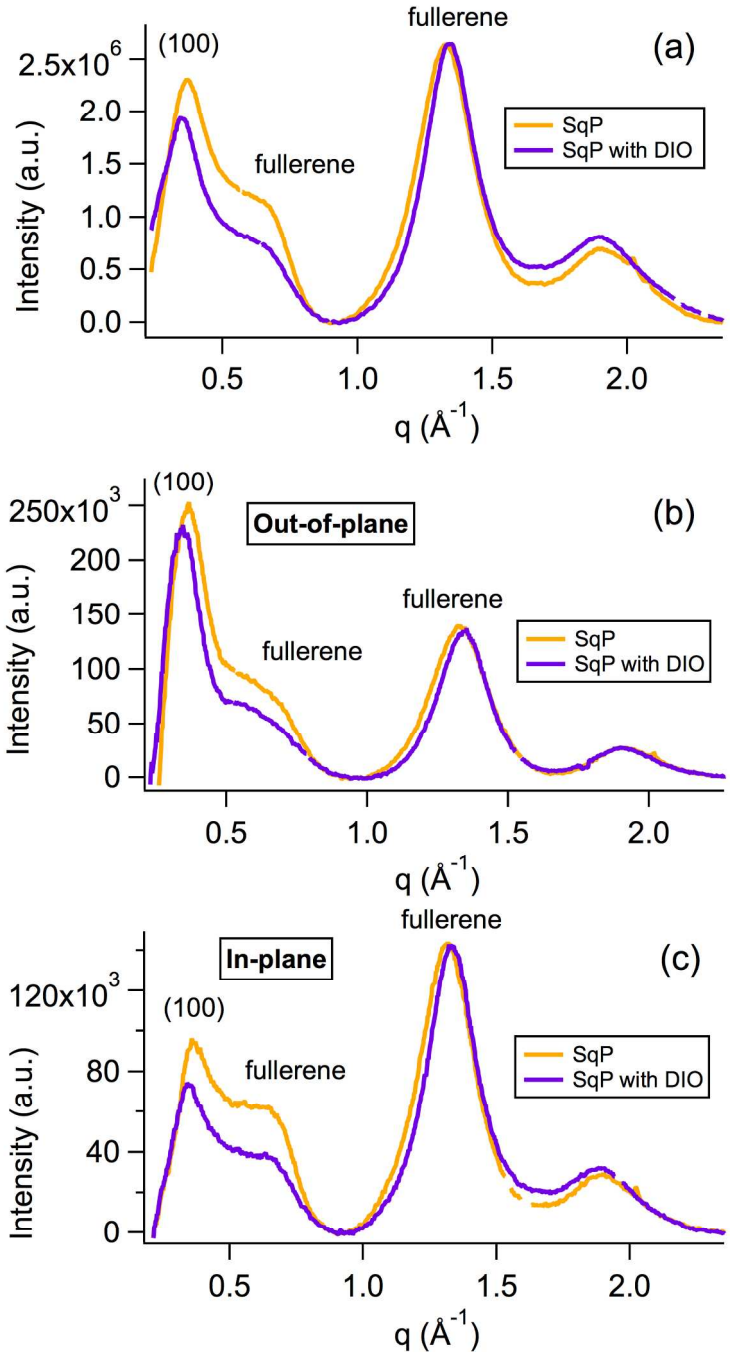

Figure S3. (a) Full integration of GIWAXS diffractograms for sequentially processed (SqP) PBDTTT-C:PCBM films, where the orange curves have no additive and the purple curves have 3% DIO in the polymer casting solution. The very strong fullerene scattering, makes the (010) diffraction peak invisible in both the (b) out-of-plane and (c) in-plane directions.

VI. Determination of PBDTTT-C:$PC_{71}BM$ weight ratio in SqP active layer via redissolving

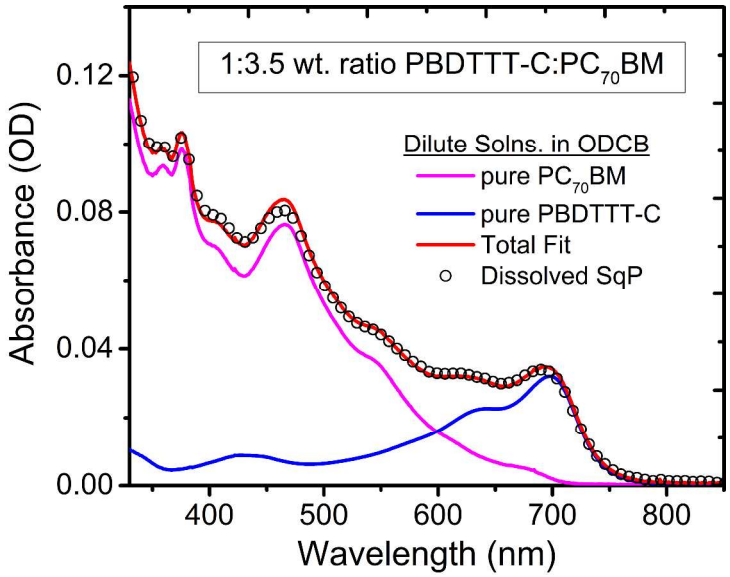

Figure S4. Solution-phase absorption spectrum (black circles) of a redissolved optimized sequentially processed device (obtained from the procedure described in Ref. 24), along with its fit to a linear combination of the pure solution-phase PBDTTT-C (blue curve) and $PC_{71}BM$ (pink curve) components. The overall weight ratio obtained from the fitting coefficients was 1:3.5 of polymer to fullerene by weight, indicating a fullerene rich device. This result is consistent with increased fullerene peak in the diffraction and EQE data.

VII. Absorbance and photoluminescence (PL) of pure, BC and SqP films

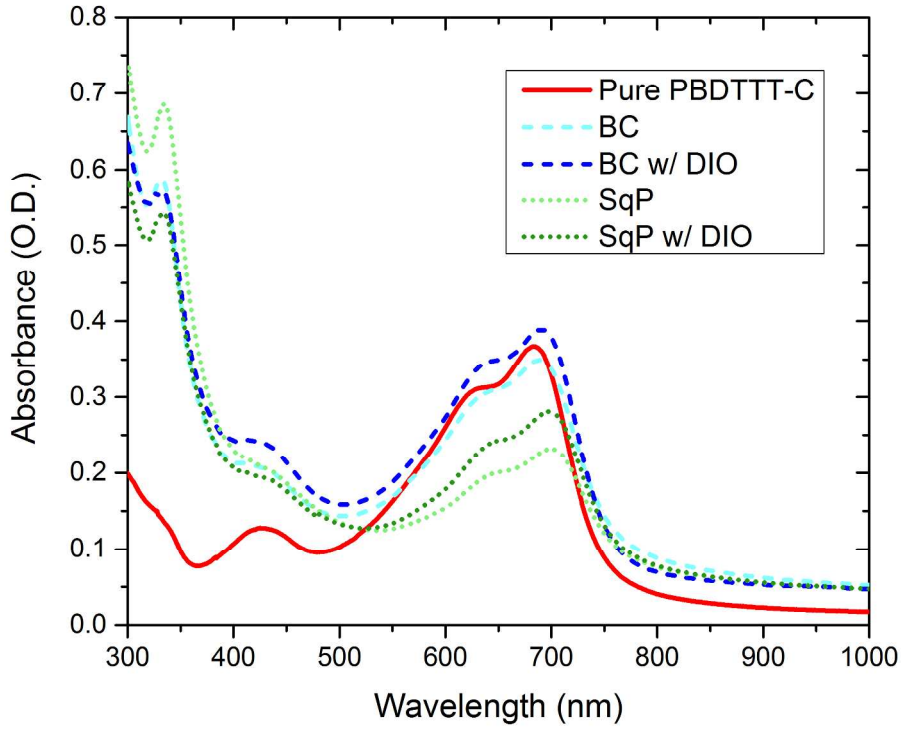

Figure S5. Absorbance of films made from pure PBDTTT-C (red solid), and BHJs made via BC with DIO (dark blue dash), without DIO (light blue dash), SqP with DIO (dark green dot) and SqP without DIO (light green dot).

VIII. SCLC mobilities

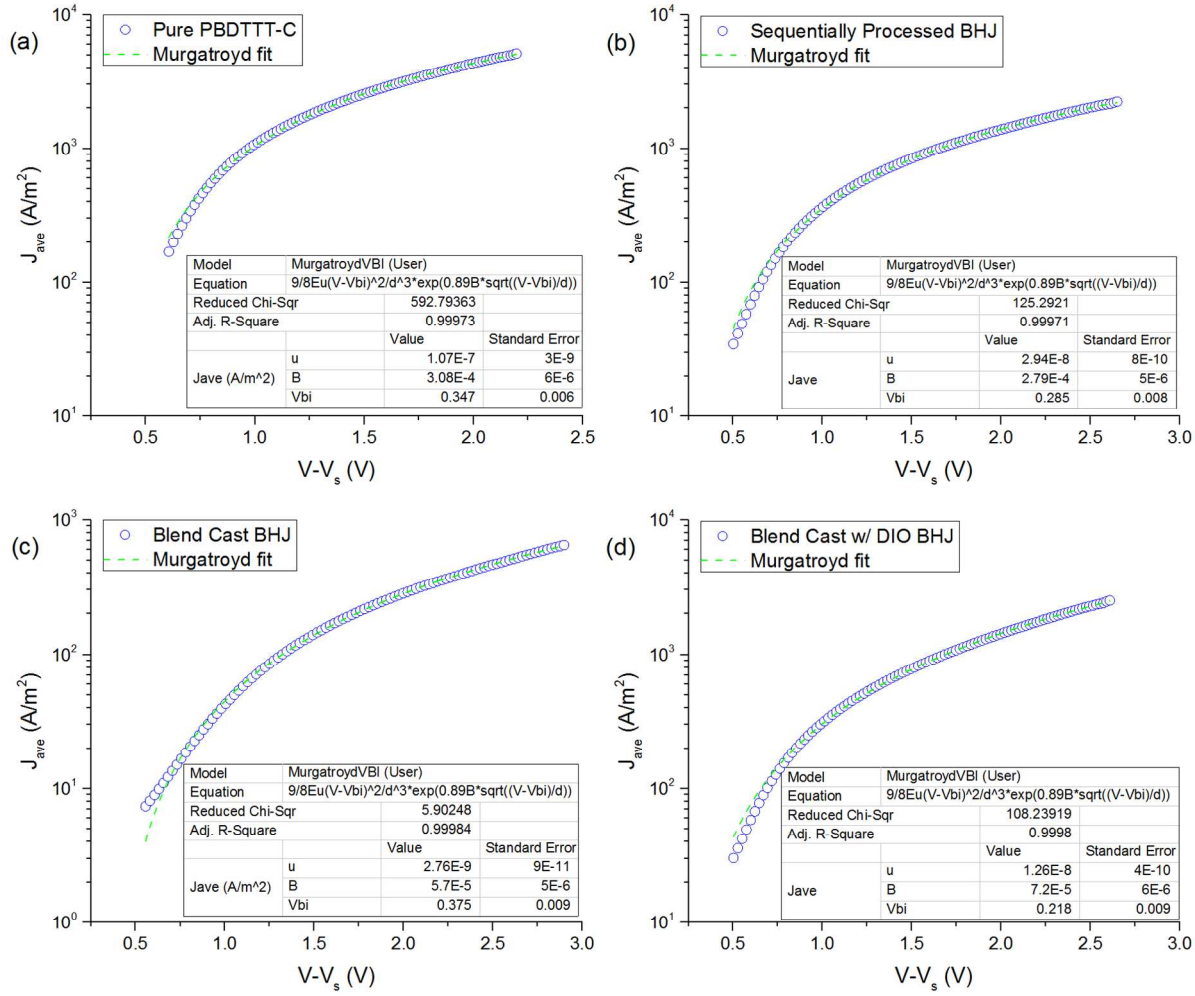

Figure S6. Current-voltage curves of hole only devices with pure PBDTTT-C (a), optimized sequentially processed PBDTTT-C:$PC_{71}BM$ (no DIO, no MeOH wash) (b), blend cast PBDTTT-C:$PC_{71}BM$ without DIO (c), and optimized blend cast PBDTTT-C:$PC_{71}BM$ (with DIO and MeOH wash). Symbols represent experimental data and the solid lines represent fit of the experimental data, performed for space charge limited current with the Murgatroyd equation: $J = \frac{9}{8}\varepsilon\mu\frac{V^2}{d^3}e^{0.89\beta\sqrt{V/d}}$. The mobilities of holes and electrons are thus extracted as fit parameters from the current-voltage curves.

IX. Device optimization of SqP with DIO in polymer/fullerene layer

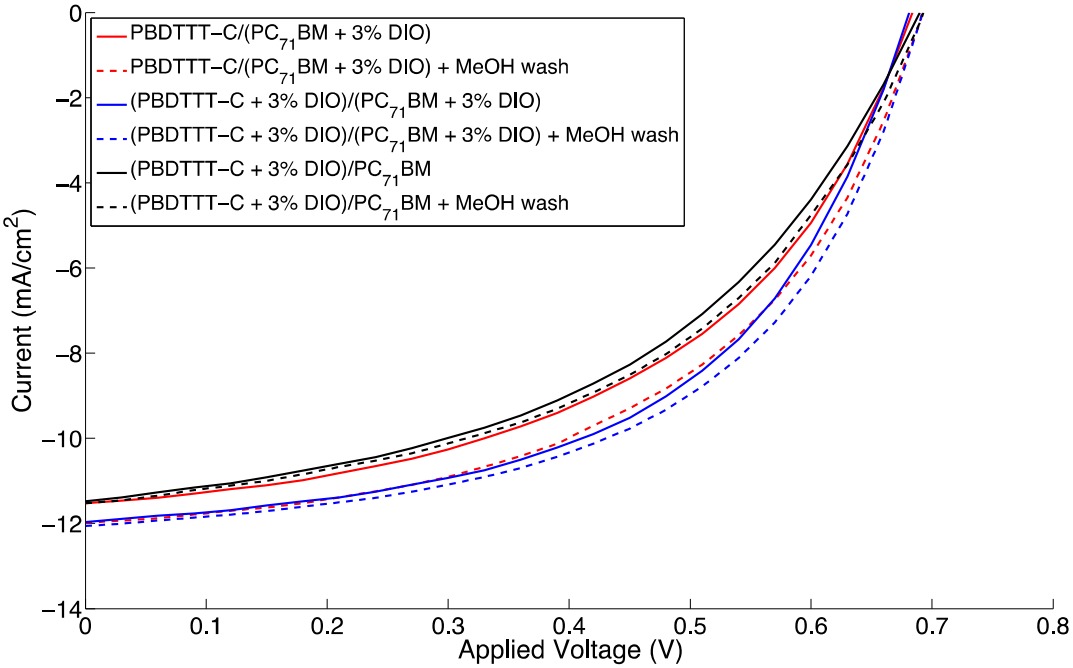

Figure S7. *J-V* device curves for sequentially processed PBDTTT-C films with DIO additive in the fullerene layer (solid red) the polymer layer (solid black) and both the fullerene and polymer layers (solid blue). Slight improvement is seen with methanol washing the DIO films (dotted). All devices have the structure: ITO/PEDOT:PSS/PBDTTT-C:$BC_{71}BM$:Ca/Al with DIO added in the indicated layers.

Table S2. Summary of *J-V* Characteristics for the PBDTTT-C devices shown in Figure S3.

Device	V_{oc} (V)	J_{sc} (mA/cm^2)	FF (%)	PCE (%)
PBDTTT-C / ($PC_{71}BM$ + 3% DIO)	0.684 ± 0.002	-11.5 ± 0.4	49 ± 1	3.9 ± 0.2
PBDTTT-C / ($PC_{71}BM$ + 3% DIO) + MeOH wash	0.692 ± 0.005	-12.0 ± 0.4	51 ± 1	4.3 ± 0.2
(PBDTTT-C + 3% DIO) / ($PC_{71}BM$ + 3% DIO)	0.681 ± 0.02	-12.0 ± 0.3	53 ± 2	4.5 ± 0.2
(PBDTTT-C + 3% DIO) / ($PC_{71}BM$ + 3% DIO) + MeOH wash	0.691 ± 0.008	-11.5 ± 0.2	53.8 ± 0.4	4.4 ± 0.2
(PBDTTT-C + 3% DIO) / $PC_{71}BM$	0.690 ± 0.003	-11.5 ± 0.2	47.0 ± 0.7	3.7 ± 0.1
(PBDTTT-C + 3% DIO) / $PC_{71}BM$ + MeOH wash	0.693 ± 0.007	-11.5 ± 0.2	48 ± 2	3.9 ± 0.2